81st International Scientific
Conference of the
University of Latvia 2023

GEODYNAMICS AND GEOSPATIAL RESEARCH

CONFERENCE PAPERS

Riga, June 1st, 2023

UNIVERSITY
OF LATVIA

81th International Scientific Conference of the University of Latvia. Geodynamics and Geospatial Research. Conference Papers. Riga, University of Latvia, 2023. 31 p.

The conference “Geodynamics and Geospatial Research” organized by the Institute of Geodesy and Geoinformatics of the University of Latvia addresses a wide range of scientific studies and is focused on the interdisciplinarity, versatility and possibilities of research in this wider context in the future to reach more significant discoveries, including business applications and innovations in solutions for commercial enterprises. The research presented at the conference is at different stages of its development and presents the achievements and the intended future. The publication is intended for researchers, students and research social partners as a source of current information and an invitation to join and support these studies.

Editor in Chief and Chair of the Conference:
Dr. sc. ing. Ingus Mitrofanovs

Publisher: University of Latvia Press
Layout designer: Ineta Priga

ISBN 978-9934-36-034-3 (PDF)
https://doi.org/10.22364/iscul.81.ggr

PREFACE

The Institute of Geodesy and Geoinformatics of the University of Latvia (LU GGI) are hard working since the reestablishment of the Institute of Geodesy in 1994. The researchers of the Institute of Geodesy (1924–1944) concentrated on the research and education in many advanced topics of that time – development and adjustment of National Geodetic networks, photogrammetry, studies of vertical Earth movement and research in gravimetric and magnetic measurements. Currently the research areas are developed in satellite geodesy and geoinformatics. In this context the main topic of LU GGI activities is concentrated on development of satellite laser ranging systems (SLR), both the hardware and control software, two SLR prototypes were developed until 2010 and the third most improved model is in the final stage of development and observation tests have been started.

The light weight and portable digital zenith camera for studies of vertical deflection has been developed at LU GGI. The test results reach precision of 0.1 arc second which is very promising for the improvement of the quality of the National model of Latvia gravity field modelling. The recent version of the National gravity field developed at the LU GGI has achieved precision of about 2 cm which is much higher than previous model (7–8 cm) used in Latvia. The high precision gravity field model is very important for practice. This reaches correspondingly high precision of normal height determination using Global Navigation Satellite systems (GNSS) in geodetic measurements. This support studies of vertical and horizontal motion of the Earth in Latvia by carrying out the analysis of the GNSS observations at the LatPos and EUPOS-RIGA permanent station networks and LU GGI GNSS stations. These studies provide high quality data for GIS data base development and for digital terrain models of Latvia in general and particular cities of Latvia.

The Institute of Geodesy and Geoinformation is substantial research and development unit of the University of Latvia. The Institutes research activities are organized in two departments – Department of Geodesy and Department of Geoinformation. Within the Department of Geodesy, the major topics of the activities are concentrated on construction of Satellite laser ranging systems (hardware, software), GNSS applications and substantial for developments is participation in the project EUPOS®. Department of Geoinformation is developing 2D and 3D country-wide geographical databases, large urban geographical databases and DEM, and developing highly detailed local geographical databases. Besides the Department of Geodesy has experienced staff dealing with satellite on ground observations.

The LU GGI research is well-known in the professional field in the world, but in Latvia it is an institution that unites and involves leading researchers from all over the country, regardless of their primal work and has become a sort of informal coordinating centre for research in this field. The high scientific quality and applied nature of many studies, presented at this conference, should be highlighted, which will allow to use in the economy this knowledge and numerous scientific solutions already in the next few years.

Director of the Institute of Geodesy and Geoinformatics
Dr. sc. ing. Ingus Mitrofanovs
June 1st, 2023.

TABLE OF CONTENTS

GNSS OBSERVATION REDUCTION DATA AT THE INSTITUTE OF GEODESY AND GEOINFORMATICS

Jānis Balodis

University of Latvia, Institute of Geodesy and Geoinformatics, Jelgavas str. 3, Riga, Latvia
E-mail: janis.balodis@lu.lv

The objective of this presentation will be the discussion on GNSS observation data reduction history at the Institute of Geodesy and Geoinformatics (GGI), shortly on the achieved research results and on the big data that is just partly investigated yet.

The Global Navigation Satellite System (GNSS) observation reduction has been performed at the Institute of Geodesy and Geoinformatics since 2007, i.e., the epoch when Latvian Continuously Operating Reference Stations (CORS) became operational. Two CORS systems LatPos [5] and EUPOS©-RIGA [7, 12] were available for GNSS static and Real Time Kinematic (RTK) observations [8]. The daily observation reduction were performed for each Latvian CORS station by using the internationally recognized methodology of Bernese software. Additionally, the observations of International GNSS Service (IGS) station Riga 1084 were reduced. The GNSS observation reduction was computed in framework of European Permanent Network (EPN) and results were sent to EUPOS© coordination centre in Hungary. There the results were collected from all the EUPOS© participating countries, validated and applied for the European Reference Framework (EUREF) densification and for European Plate Observing System (EPOS).

The GNSS static observations were carried out in 4 hour observation sessions at the 1st order levelling points within the studies of Latvian quasi-geoid modelling projects in GGI [9, 10, 11]. The observations were reduced in framework of ETRS89 coordinate system by using the Bernese 5.2 software. The ellipsoidal heights of the levelling benchmarks were tied to the normal heights of National levelling network by using the Helmert 7-parameter transformation. As result 409 GPS/Levelling point data were tied to the Latvian national height system and used by GGI researchers for the national quasi-geoid development. The residuals of Helmert transformation adjustment are depicted in Fig.1 that can be interpreted to some extent as a map of normal height discrepancies in National 1st order levelling network.

It is seen that uplift occurred on the coast line of Riga Bay and near Ventspils at the coast of Baltic Sea [6, 13]. Land subsidence observed in several patches of adjacent benchmarhs in middle of country (Madona, Pļaviņas, Jēkabpils, Viesīte, Jelgava, Priekule Kurzemē).

The Deflection of vertical (DoV) measurements were obtained at the GGI by using the original Digital Zenith Camera (DZC) developed by the GGI scientists A. Zarins, A. Rubans and others [1, 2, 14, 15, 16]. About 400 DoV measurements cover the territory of Latvia.

In 2020 in framework of Programme for European Cooperating States (PECS), European Space Agency Contract No: 4000128661/19/NL/SC, project "Ionospheric characterization by statistics analysis of Latvian GBAS 11-year selective daily observations" were performed the studies of space weather impact to Latvian CORS selective positioning results [3, 4]. The main objective of this study was to obtain the Latvian CORS observation 90-sec kinematic post-processing solutions by Bernese v 5.2 GNSS software, to perform analysis of the space weather impact. 36.7 million positioning solutions obtained for ionospheric scintillation analysis. However, just 0.6% of results occurred to be disturbed solutions with positioning discrepancies of more than 10 cm and just these solutions were analyzed. 99.4% of obtained 90-sec kinematic solutions were not analyzed yet. Up to 30 software program modules were developed in Fortran g95, C++ and Python programming languages. Whole the space weather research data contains about 15 Gb space on the computer disk.

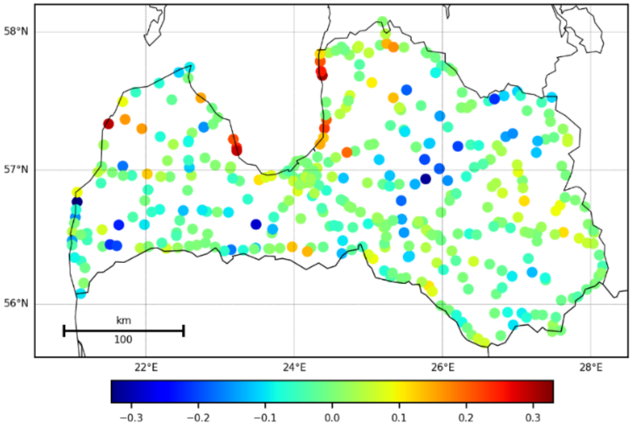

Fig. 1. Schematic map of the normal height discrepancies resulted from 4 hour GNSS static measurements (map designed by I.Vārna)

Several PhD students in GGI have used the fragmented data sets for their dissertation development. Many global data sets on the space research and on Earth and atmosphere physics are available in NASA and in other publicly available data bases.

References

[1] Abele, M., Balodis, J., Rubans, A., Silabriedis, G. (2004). Project on the Automated Digital Camera for Vertical Deflection Determination. International Symposium EUREF – 2004. Bratislava, June 2–5, 2004. http://www.euref-iag.net/symposia/symposia_2004_Bratislava.html

[2] Abele, M., Balodis, J., Janpaule, I., Lasmane, I., Rubans, A., Zariņš, A. (2012). Digital Zenith Camera for Vertical Deflection Determination. *Geodesy and Cartography, Taylor & Francis, 38*(4), 123–129. Vilnius Gediminas University. ISSN 2029-6991.

[3] Balodis, J., Normand, M., Varna, I. (2021). Extreme Solar Events' Impact on GPS Positioning Results. *Remote Sensing, 13*(3624). https://doi.org/10.3390/rs13183624.

[4] Balodis, J., Normand, M., Zarins, A. (2023). The Movement of GPS Positioning Discrepancy Clouds at a Mid-Latitude Region in March 2015'. *Remote Sensing, 15*(8), 2032. https://doi.org/10.3390/rs15082032

[5] Haritonova, D., Balodis, J., Janpaule, I., Normand, M. (2013). Displacements at the GNSS Stations. *Civil Engineering' 13. 4th International Scientific Conference Proceedings*, Vol. 4, pp. 305.–309. Jelgava, Latvia University of Agriculture. ISSN 2255-7776.

[6] Haritonova, D. (2021). Non-tidal loading of the Baltic Sea in Latvian GNSS time series. *Journal of Applied Geodesy*, 1–12. https://doi.org/10.1515/jag-2021-0024.

[7] Janpaule, I., Caunite, M., Balodis, J., Silabriedis, G. (2009). *EUPOS®* Network Solution. *Proceedings of the International Symposium on Global Navigation Satellite Systems, Space-based and Ground-based*

Augmentation Systems and Applications, pp. 61–67. Berlin (Germany), 1–2 December, 2009. ISBN 978-3-938373-93-4.

[8] Magiera, W., Vārna, I., Mitrofanovs, I., Silabriedis, G., Krawczyk, A., Skorupa, B., Apollo, M., Maciuk, K. (2022). Accuracy of Code GNSS Receivers under Various Conditions. *Remote Sensing, 14*(11), 26152615. https://doi.org/10.3390/rs14112615. ISSN 2072-4292.

[9] Morozova, K., Balodis, J., Zariņš, A., Rubans, A. and Jager, R. (2017). Digital zenith cameras results and its use in DFHRS v. 4.3 software for quasi-geoid determination. *Proceedings – 2017 Baltic Geodetic Congress (Geomatics)*, pp. 174–178. https://doi.org/10.1109/BGC.Geomatics.2017.74.

[10] Morozova, K., Jäger, R., Zarins, A., Balodis, J., Varna, I., Silabriedis, G. (2021). Evaluation of quasi-geoid model based on astrogeodetic measurements: case of Latvia. *Journal of Applied Geodesy, 15*(4), 319–327. https://doi.org/10.1515/jag-2021-0030. ERDF project No. 1.1.1.1/16/A/160.

[11] Morozova, K., Jäger, R., Balodis, J., Silabriedis, G., Kaminskis, J., Kalinka, M., Balodis, K., Mitrofanovs, I. (2019). Preliminary results on qgeoid for Western part of Latvia using Digital-Zenith Camera and DFHRS V.4.3 Software. *Geophysica, 54*(1), 61–68.

[12] Silabriedis, G., Plotnikov, S., Balodis, J., Caunite, M., Zelinska, E. (2008). The EUPOS-Riga Application for Mapping Control. 3rd International Conference and 3rd International Trade Fair of Geodesy, Cartography, Navigation and Geoinformatics GEOS 2008. Prague, 27th–28th February 2008. *Conference Proceedings. Research Institute of Geodesy, Topography and Cartography*. Vol. 54, Publication No. 44. ISBN 978-80-5881-29-5. Abstract. P. 5. Full text: www.vugtk.cz/geos/2008

[13] Vārna, I., Haritonova, D., Balodis, J. (2019). Velocity Fields of the Latvian CORS Station Daily Coordinates for 2012–2017. *Geophysica, 54*(1), 137–144.

[14] Zariņš, A., Haritonova, D., Rubans, A., Silabriedis, G. and Zvirgzds, J. (2016). Field tests of astrometric subsystem. *Geodesy and Cartography, 42*(1), 1–6. https://doi.org/10.3846/20296991.2016.1168029

[15] Zariņš, A., Rubans, A. and Silabriedis, G. (2016). Digital zenith camera of the University of Latvia. *Geodesy and Cartography, 42*(4), 129–135. https://doi.org/10.3846/20296991.2016.1268434

[16] Zariņš, A., Rubans, A. and Silabriedis, G. (2018). Performance analysis of Latvian zenith camera. *Geodesy and Cartography, 44*(1), 1–5. https://doi.org/10.3846/gac.2018.876

GLOBAL DISASTERS: AN HISTORICAL ANALYSIS AND PREDICTION

Julia Buszta, Katarzyna Wójcik, Kamil Maciuk

AGH University of Science and Technology, Krakow, Poland
E-mail: maciuk@agh.edu.pl

The world is still experiencing a number of natural disasters that have had a serious impact on people's lives and the environment. In recent years, mainly through climate change and global warming, the scale and frequency of such phenomena has been increasing. Examples from recent years include the China earthquake in 2008 (magnitude of 7.9 on the Richter scale struck on the Sichuan province) or Hurricane Sandy in 2012 (more than 80,000 people died, one of the largest hurricanes ever to hit the east coast of the United States, estimated damages cost have been more than $70 billion).

This paper analyses 8 natural disasters over the last 60 years (1960–2018) divided by the continents, the number of natural disasters in relation to population and the number of natural disasters per continent area. In addition, the prediction of the number of individual natural disasters was determined using polynomial analysis for next 20 years. Figure 1 shows the distribution of natural disasters on continents per 1 million citizens and per 1000 square kilometres. It shows a great advantages of areas and people affected in the less developed countries.

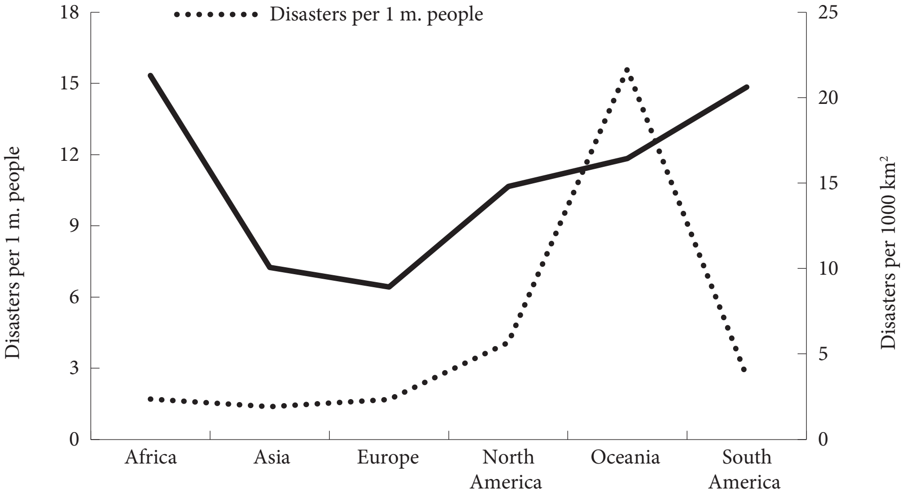

Fig. 1. Distribution of natural disaster among continents per people and per are

Authors in detail analysed distribution of each natural disaster on the continents and created a cartodiagrams based on 5-class classification for each disaster separately. Figure 2 shows example distribution of the floods in the analyzed period. It in a simple way showing a countries affected during 60 years by each disaster most.

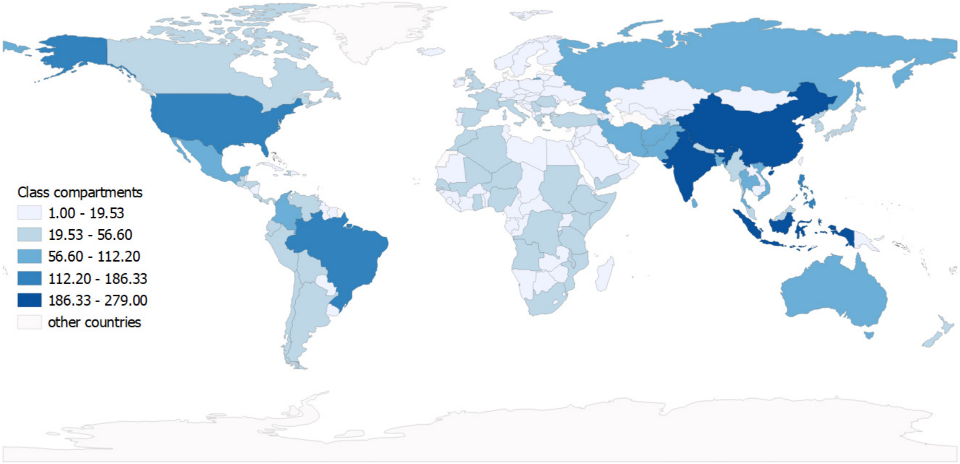

Fig. 2. Numbers of floods distributed by countries

Except spatiotemporal distribution authors also prepared a 20-years forecasting of the appearances of the disaster globally. Figure 3 shows number of storms in analysed period with a 20-years forecast.

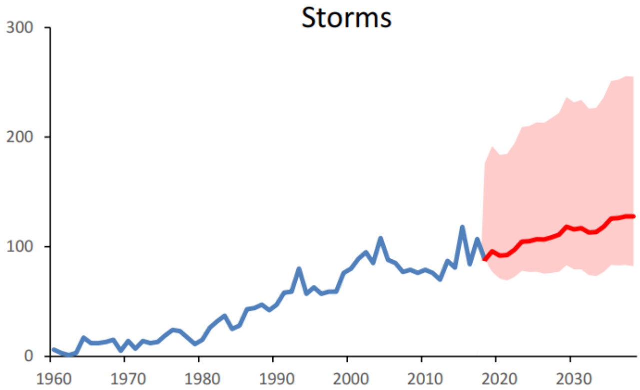

Fig. 3. Disasters charts from 1960-2018 with forecasts for the next 20 years

As result authors showed a number of appearances of each disaster in each continent, countries affected by it most and a future trends.

RELIABILITY OF OUTLIERS AND THEIR EVOLUTION IN GNSS CLOCK PRODUCTS

Kamil Maciuk[1], **Inese Varna**[2], **Karolina Krzykowska-Piotrowska**[3]

[1] *Department of Integrated Geodesy and Cartography, AGH University of Science and Technology, al. Mickiewicza 30, 30-059 Krakow, Poland*

[2] *Institute of Geodesy and Geoinformatics, University of Latvia, Jelgavas street 3, LV-1004, Riga, Latvia*

[3] *Faculty of Transport, Warsaw University of Technology, ul. Koszykowa 75, 00-662 Warsaw, Poland*

E-mail: maciuk@agh.edu.pl

Time is crucial in GNSS (Global Navigation Satellite System) systems such as GPS, GLONASS, Galileo and Beidou, it is measured with a high precision, enabling accurate position of the receiver. Thus receiver's clock must be very accurate to enable accurate position and a number of error-producing factors (e.g. multipath, atmosphere impact) must be included into processing.. Time and/or accurate position determination is important in many fields such as navigation, surveying, meteorology and even in finance.

In this presentation authors analysed a number of clock correction products in terms of number and magnitude of outlier observations in four GNSS systems based on final MGEX products for the years 2014–2021. Among this time there where available 120 satellites: 37 Beidou, 26 Galileo, 32 GPS and 25 GLONASS satellites. Authors analysed phase, frequency and noise data. Figure 1 shows a sample raw phase data of selected satellites, which shows a different change and nature of clock correction course in time, e.g. line, polynomial, random etc.

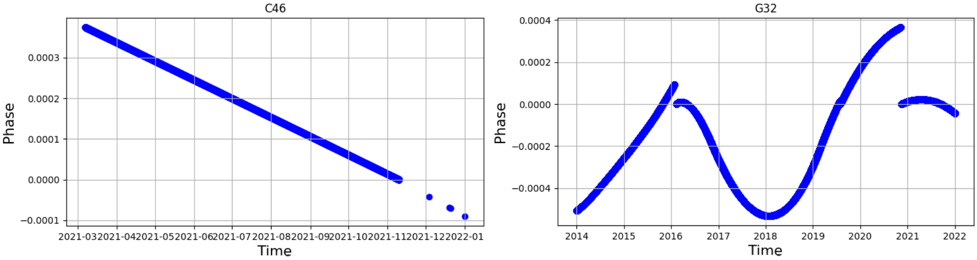

Fig. 1. Phase data of selected satellites: C46 (Beidou) and G32 (GPS)

First derivate of the phase in time is a frequency (Figure 2), which allows to see a quite different nature of the graphs courses between GNSS systems, satellite blocks and between clocks types.

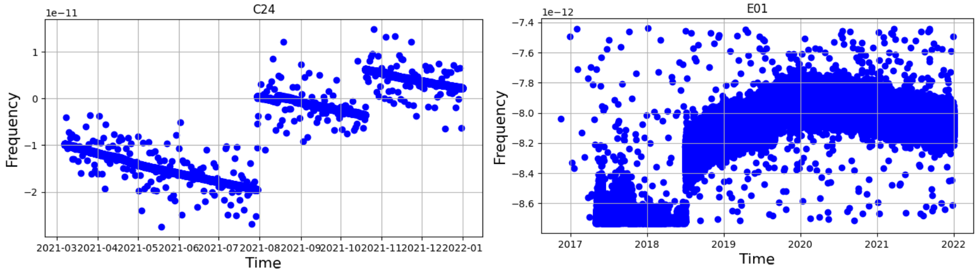

Fig. 2. Frequency data of selected satellites: C24 (Beidou) and E01 (Galileo)

The Allan deviation (ADEV) and it's modificated version allows for determine a noise characteristic for analysed time series and it is a common tool for atomic clock stabilities analyses. Figure 3 shows the HDEV (Hadamard deviation, modificated version of ADEV) of selected satellites, which allows for detect based of the graph course noise type characteristic for selected satellites and its intervals. Figure 4 is similar to Figure 3, but allows for comparison HDEV changes year-to-year.

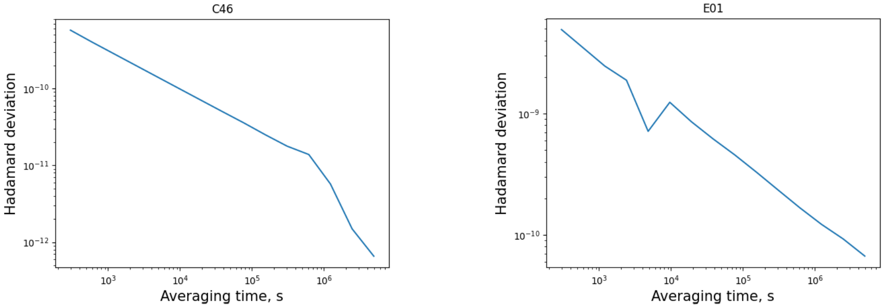

Fig. 3. Yearly Hadamard deviation of selected satellites: C46 (Beidou) and E01 (Galileo)

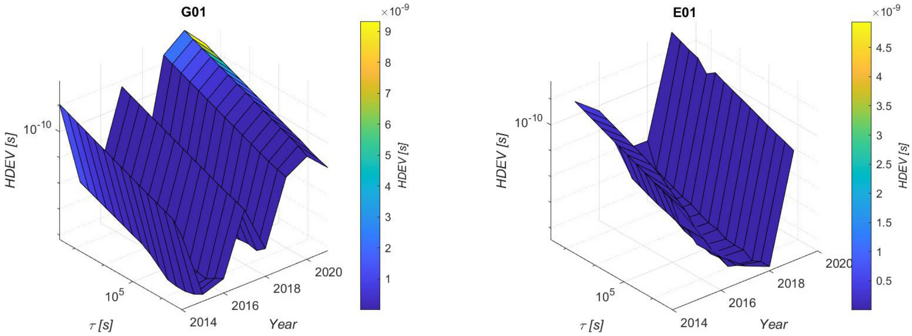

Fig. 4. Multidimensional Hadamard deviation selected satellites: C46 (Beidou) and G32 (GPS)

As results authors find a couple of new phenomena, e.g. stability of the GPS and GLONASS systems (in general) are better than the BeiDou and Galileo systems, which means that repeatability of the clock corrections are more consistent in time.

THE MOVEMENT OF GPS POSITIONING DISCREPANCY CLOUDS AT A MID-LATITUDE REGION IN MARCH 2015

Madara Normand[1,2]**, Janis Balodis**[1]**, Ansis Zarins**[1]

[1] *University of Latvia, Institute of Geodesy and Geoinformatics, Jelgavas str. 3, Riga, Latvia*
[2] *Department of Geomatics, Riga Technical University, Kipsalas str. 6A, Riga, Latvia*
E-mail: madara.normanda@lu.lv

Space weather nowadays has become a challenging subject in many global navigation satellite systems (GNSS) applications. We introduce a new term *discrepancy clouds* when analyzing the nature of irregularities of the ionospheric scintillation's disturbed positioning results along with a new methodology to discover the space weather impact on Latvian Continuously Operating Reference Stations (CORS) and six selected European Geostationary Navigation Overlay Service (EGNOS) ground-based Ranging and Integrity Monitoring Stations (RIMS) global positioning system (GPS) positioning results at a mid-latitude region in March 2015. St. Patrick's day storm in this month was the first super geomagnetic storm during the 24th Solar Cycle.

Methodology and theoretical orientation

To predict ionospheric characteristics, it is effective to use models considering the state of the ionosphere in the past, as well as the history of parameters characterizing the main impact on the ionosphere from above – solar and magnetic activity [1]. GPS 90 s observation data firstly was post-processed with Bernese GNSS Software v5.2. For the analysis of the post-processed data, software programs in Fortran g95, C++, and Phyton programming languages, developed at LU GGI were used. Data was divided in subsets. For data analysis and the data structure statement Formulas (1)–(8) were formed in the expressions of mathematical logic and set theory on the basis of [2]. The whole set of information was denoted by set T. The subset S of Latvian CORS stations was denoted by their DOMES names (s_j), where the count of stations (cardinality of set S) was 30 for March 2015 (Formula (1)).

$$S \coloneqq \{\langle s_j, \varphi_j, \lambda_j\rangle : 1 \leq j \leq 30\} \tag{1}$$

Here, the station's name (DOME) is s, latitude is φ, and longitude is λ.

Each subset p_i ($1 \leq i \leq 1584$), denoted as a *discrepancy cloud* (subset of stations where discrepancies occurred simultaneously), is described as a subset in Formula (2). The cardinality of the whole set of clouds in March was 1584.

$$p_i \coloneqq \{\langle s_{ij}\rangle : j \in \langle D_i, t_i\rangle, n_i \in \langle D_i, t_i\rangle, 1 \leq j \leq n_i\} \tag{2}$$

Where Day D_i (31 days in March), time t_i, cardinality n_i

The subset of cloud discrepancy w_i (Formula (3)) is describing data content. The union (4) of all 1584 discrepancy subsets represents the information of the positioning-degraded results.

$$w_i \coloneqq \{\langle k_i, D_i, t_i, s_{ij}, d_{ij}, r_{ij}\rangle : j \in \langle D_i, t_i\rangle, n_i \in \langle D_i, t_i\rangle, 1 \leq j \leq n_i\} \tag{3}$$

$$W \coloneqq \cup \{w_i, 1 \leq i \leq 1584\} \tag{4}$$

The symbol n_i defined in Formula (5) denotes the cardinality of selected subsets described in Formulas (2) and (3).

$$N \coloneqq \{n_i : n_i \in |p_i|, 1 \leq i \leq 1584\} \tag{5}$$

Both the cloud (or subset of stations) p_i and cloud discrepancy information w_i are connected with a corresponding record number k_i, date, time t_i, and count of stations in each subset p_i.

Subset P of Formula (6) denotes the union of all 36 peak subsets. On each day D_i, there was one subset with max station cardinality (Formula (6)). The max occurrence subsets were different for each day of the month.

$$P \coloneqq \cup \{\langle k_i, D_i, t_i, p_i, d_{ij}, r_{ij}\rangle : j \in \langle D_i, t_i\rangle, j \leq n_i, n_i = max \in D_i\} \tag{6}$$

The daily peak subsets for each 'calm' day in March were very similar to each other, occurring approximately after midnight in predawn time, except for 17 March. The subsets p_i contained the site names of stations s_{ij}, where faulty positioning solutions occurred with discrepancies d_{ij} (summary error) and ROTI values r_{ij} for these exact sites at this exact event time t_i.

On each day, there were occasions where several clouds followed each other every 90 s (1.5 min). The subset of adjacent clouds were named batches and denoted by b_i for each day "i". In each batch b_i (Formula (7)), there were various numbers of clouds described by Formulas (3)–(5).

However, on the day of the geomagnetic storms, there was more than one batch; therefore, on this day, instead of one batch, a group of batches was considered. The group of batches was just on 17 March. The subsets b_i (batches of clouds) contained subsets (records) p_{ij} with numerical auxiliary k_{ij} on the fixed date D_i, time events t_{jj}, and discrepancies d_{ij}, which are subsets $b_i \in B$ (Formula (7)). The batches were counted only in situations when the adjacent subsets p_{ij} occurred simultaneously in three or more stations.

$$b_i \coloneqq \cup \{\langle k_{ij}, D_i, t_{k_{ij}}, p_{k_{ij}}, w_{k_{ij}}\rangle : \exists\ k_{ij} \in D_i, \exists\ t_{k_{ij}} \in D_i, \exists\ t_{k_{ij}+1} \in D_i, (t_{k_{ij}+1} - t_{k_{ij}}) \leq 90\ sec, n_{ik_{ij}} \geq 3\} \tag{7}$$

For each day "i" subset b_i is the union of subsets of various sizes containing cloud information of corresponding days, resulting in cardinality $|b_i|$. There were 32 batches of clouds in March 2015, and two of them on 17 March. The union of batches (8) was denoted by B.

$$B \coloneqq \cup \{b_i, 1 \leq i \leq 32\} \tag{8}$$

Further analysis was performed in three data divisions: cloud batches (subsets $B \in T$), 36 selected peak clouds (subsets $P \in T$), and 36 subsets of adjacent 5-cloud groups ($P' \in T$), where the peak cloud was the central one. These groups were denoted by B, P, and P'. The subset relationships are described by Formula (9).

$$P \subset P' \subset B \subset T \tag{9}$$

For selected batches b_i, the discrepancy scatter plots for sample subsets W with a discrepancy size proportional to the logarithm of the Up component discrepancies were designed in order to validate the discrepancies' distribution in adjacent 90 s (1.5 min) time events t_k.

For peak subsets P, Pearson's correlation coefficient was computed to find the relationship between discrepancies (subset d_{ij}) and the ROTI (subset r_{ij}) by using d_{ij}, r_{ij} instead of x_j, y_j in Pearson's correlation Equation.

For peak subsets of P, the intersection of the peak on 1 March (subset p_1) with 35 other peaks was performed in order to find the commonly impacted stations. The intersection is described by Formula (10).

$$c_v \coloneqq \{\langle s\_{}_{1j}\rangle \cap \langle s_{vl}\rangle : \exists\, s_{1j} \in p_1, \exists\, s_{vl} \in p_v, 1 \leq j \leq n_1, 1 \leq \mathrm{l} \leq n_v, 2 \leq v \leq 36\} \qquad (10)$$

From batch subsets B, Pearson's coefficients were computed using Person's correlation Equation for the relationship between $d_{1j} \in w_1$ and $d_{vj} \in w_v$ for subsets of all stations $s_{vj} \in c_v$ from Formula (10).

For subset B stations, the monthly mean discrepancies and standard deviations were computed for each station in two groups: (1) of all peak subsets on 'calm' days (C) and (2) 'storm' day (S), correspondingly. The count of faulty solutions for each station in both situations was performed.

For cloud groups of subset P', the five adjacent clouds, as a part of the daily cloud batches, were selected from the set T'. These were chosen as two subsets before the peak and two after the peak (in addition to the peak subset) to study the movement of adjacent discrepancy clouds within each day.

For the group of subset P', the intersection was performed for subsets of stations within each of group.

The cloud center coordinates were computed by computing the mean geographical coordinates for a subset of stations in various combinations.

The GPS data on 18 March 2015 from EGNOS ground-based RIMS stations GVLA, GVLB, LAPA, LAPB, WRSA, and WRSB were analyzed as well.

Findings

- Each daily ionospheric scintillation intensity maximum appeared about 4 min 8 s earlier than the previous day. Such regularity might indicate an inertial (not rotating together with the Earth) location of the source of disturbances, with a corresponding position of a zero-meridian plane close to 150° East for 1 March. However, the source clearly was not of a cosmological origin—the daily time shift was 12 s, which is too long for the exact compensation of the Earth's rotation. Right ascension is slowly changing, decreasing at a rate of about 18 degrees per year (full rotation in 20 years).
- All regular disturbance batches exhibited a fairly similar picture: the onset occurred within 5–10 min, all territory was affected simultaneously, and no noticeable signs of motion were present in the affected area. The maximum number of disturbed sites occurred a few minutes after the maximum disturbance intensity; it is likely some sites were able to withstand the disturbing factors longer than others. The duration of a strong disturbance did not exceed 5 min. On 17 March, in addition to the regular disturbance batch, a second, much longer (3 h), but weaker disturbance wave was present. Presumably, it was connected to a geomagnetic storm. The onset was gradual and took almost an hour. After that, a stable high level of disturbance continued for about 2 h. The distribution of affected sites was similar to the regular batches.
- During the geomagnetic storm on 17 March, loss of lock occurred in 20 stations. In 10 irregularly spread sites, loss of lock did not occur.

- The fluctuation of the discrepancies during the St. Patrick's Day geomagnetic storm in meters were as follows for Northing [–130.511; 106.922], Easting [–74.896; 120.517], and Up [–531.624; 154.625].
- Pearson's correlation coefficients were obtained in relation to discrepancies and ROTI in peak subsets $p_i \in B$. All correlation coefficients were less than 0.4 or below zero. This meant that the correlation of discrepancies with ROTI was weak.

In 14 cases (40%), Pearson's correlation coefficient for the peak discrepancies was > 0.4, i.e., the relationship was good. In 19 cases (55%), the relationship was weak (< 0.4), and only in two cases (5%) was the relationship negative.

- The comparison of discrepancy clouds on March 1 with the seven clouds on March 17 revealed that the percentage of common stations was < 50% at the beginning of March 17. However, the count of common stations in the peak cloud, by the end of the day, reached 100%, which fits the trend of the peak event time series for the whole month of March.
- However, the results were quite different when the intersection was performed on five clouds inside each group. The cloud subsets in each group on 'calm' days were moving and/or disappearing faster than cloud subsets on the day of the geomagnetic storm, 17 March.
- The mean values of the subsets of station coordinates were computed assuming a geometrical center of station sites in the whole peak subsets.

Table 1. Parameters of the peak cloud (P) and five-cloud (P) center coordinates

	Peak-cloud sets		**5-cloud sets March 1–16**		**5-cloud sets March 17**		**5-cloud sets March 18–31**	
	Longitude	**Latitude**	**Longitude**	**Latitude**	**Longitude**	**Latitude**	**Longitude**	**Latitude**
Mean	24.85°	56.93°	24.94°	56.93°	24.55°	56.91°	25.15°	56.95°
STD	0.29°	0.03°	0.39°	0.06°	0.23°	0.05°	0.57°	0.08°
MAX	25.32°	57.03°	26.10°	57.16°	25.09°	57.02°	26.42°	57.19°
MIN	24.38°	56.85°	24.17°	56.75°	24.13°	56.77°	24.15°	56.80°
MAX-MIN	0.94°	0.18°	1.93°	0.41°	0.96°	0.25°	2.27°	0.39°

- The mean coordinates of adjacent cloud subsets differed significantly within the framework of its batches.
- The first six out of seven groups of peaks (starting from $b_{16} \in B$) expressed the log error of station operation. They described the damage to the CORS network caused by the St. Patrick's geomagnetic storm.
- From all the 57,600 90 s solutions which were performed in the six RIMS stations, the total count of faulty solutions on 16–18 March was 3269, i.e., 5.7% of faulty solutions occurred on a geomagnetic storm impact day.
- RIMS station GVLA was in a loss of lock for almost 7 h, starting from 13:39:00, LAPA ~5 h, GVLB ~10 h, LAPB ~2 h, and WRSA ~1.5 h from ~16:15:00, GVLA ~3.5 h from 20:45, LAPA ~2 h from 20:45, and LAPB ~2 h from 22:19:30. This means that during the St. Patrick's geomagnetic storm, the data of these RIMS ground-based stations

were strongly affected by the geomagnetic storm. The duration of loss of lock for the RIMS stations was much longer compared to the Latvian CORS stations.
- The presence of peak clouds was visible for RIMS stations, similar to the discrepancy clouds of the Latvian CORS.

Conclusion

The new methodology leads us to conclude that each "shot" after 90 s gives a completely new cloud with a new impacted station subset, its configuration, and completely irregular discrepancy values. The positioning measurements were destroyed during the St. Patrick's geomagnetic storm, when most of the stations experienced a loss-of-lock situation. The size of individual station ionospheric disturbances was not predictable. They had a sporadic, random, and occasional character. The St. Patrick's Day geomagnetic storm impacted GPS receivers of various producers in space and on the ground. The three-day analysis of EGNOS ground-based RIMS station data is too short to make any conclusions. However, a 10-h loss of lock of the RIMS station in comparison with a 4-h loss of lock of the Latvian CORS network station elicits interest in looking at the behavior of RIMS stations on 'calm' days as well.

References

[1] Salimov, B. G., Berngardt, O. I., Khmelnov, A. E., Ratovsky, K. G., Kusonsky, O. A. (2023). Application of convolution neural networks for critical frequency foF2 prediction. *Solar-Terrestrial Physics, 9*(1), 56–67. https://doi.org/10.12737/stp-91202307

[2] Cīrulis, J. (2007). *Mathematical logic and set theory* (In Latvian: *Matemātiskā loģika un kopu teorija*). Riga: Zvaigzne ABC, Latvia.

MITESENS – R&D ON NAVIGATION STATE ESTIMATION, FLIGHT CONTROL, GEOREFERENCINGAND AND SLAM TASKS FOR AN AUTONOMOUS UAV SYSTEM FOR MITES-DETECTION IN THE ERA OF DIGITAL HORTICULTURE 4.0

Reiner Jäger, Felix Vortisch

University of Applied Sciences Karlsruhe (HKA), Laboratory for GNSS and Navigation,
Moltkestr. 30, D-76133 Karlsruhe,Germany.
E-mail: reiner.jaeger@web.de

The aim of the MITESENS project [1] in the Laboratory for GNSS and Navigation [2] is an UAS based monitoring system (UAS = Unmanned Aerial System with an UAV as carrier platform) for the early detection and monitoring of spider-mites on plant leaves in greenhouse cultivations [3].

The autonomous UAS flight over the plant stand is controlled with a newly developed MITESENS UAS flight control (FC). The respective hardware development for the multisensory and IEEE 1588 time-synchronized GNSS/MEMS/Optics FC box is also part of the R&D project. The FC determines out- and indoors the 18 parameters navigation state vector y(t) (3D-position, 3D-velocity, 3-accelerations, 3D-rotation rates, 3D-rotation rate changes), which is georeferenced in the ETRF89 (European Terrestrial Reference Frame 89), or generally in the ITRFyyyy.zzzz.mm, using optionally DGNSS and PPP.

In a first instance the navigation state y(t) is the essential component of the FC controlling the desired trajectory of the MITESENS UAS. As flight control FC types, the development of a PID control, and of a multi predictive control (MPC) are carried out. The PID control is used to set up the georeferenced building model (BIM) of a greenhouse from the UAS optics of the camera and/or the lidar sensor, by operating the UAS with a remote control. The MPC control is used in further for the general mission of mites detection and monitoring by the UAS being equipped also with a multi-spectral camera, where the UAS is autonomously flying out- and indoors. Indoors the UAS is using the digital twin of the greenhouse BIM model by an AI-based feature recognition vision component of the FC. AI and photogrammetry provide the position information from the ERTF89 or ITRFyyy.zz.mm BIM model instead from GNSS, in the navigation state estimation y(t) and MPC control.

Conceptionally the navigation y(t) is used not only as a reference for the FC, but y(t) also forms the common core for further computational operations. So, all images contain y(t) as metadata. A first further task of the UAS is the generation of an ERTF89 or ITRFyyy.zz.mm georeferenced 3D voxel model of the plants, typically by a bundle block adjustment or sequential SLAM of the RGB camera (ZED 2i) data with known exterior orientation as component parts of y(t). Further as the image metadata y(t) is used for the georeferencing of the acquired spectral image data for mites-detection. The acquired hyperspectral images information is on wavelengths between 500 nm to 900 nm. This image information is evaluated using again AI (XGBoost classification based on a decision tree algorithm), and on dividing the infestation probability of the leaves into three classes (green, yellow and red) with a prediction accuracy for the spider mite infestation above 85%. The classified hyperspectral metadata images are then pixelwise calculated back to the ERTF89 or ITRFyyy.zz.mm referenced 3D plant stand using y(t), and creating in that way a classified 3D voxel model. In order to realize a simple and spatially clear representation of the recorded spider mite infestation for horticultural practice, the classified 3D voxel data are converted into a 2D plan map view of the greenhouse infestation situation.

The complete MITESENS UAS is presented. The focus is on the mathematical models, algorithms and software of the out- and indoor navigation state y(t) estimation and SLAM [4], [5], the MPC based control for the autonomous flight [5], the 3D voxel model generation, and the back projection of the classified images to receive and monitor in further the classified 3D voxel model of the mite infestation. The results are of the MITSENS UAS development are shown.

References

[1] H-KA: MITESENS-WebSite. www.h-ka.de/iaf/mitesens. Karlsruhe University of Applied Sciences (HKA). 2020–2023.

[2] Jäger, R. (2000–2023). Laboratory for GNSS and Navigation. http://goca.info/Labor.GNSS.und.Navigation/index.php and www.arbeitsplatz-erde.de/profile/labor-fuer-gnss-und-navigation/.

[3] Espinoza, F., Jäger, R. (2022). UAS-System MiteSens – Spinnmilbenbefall im Unterglasanbau frühzeitig erkennen. Zeitschrift Landinfo 01/2022. www.openagrar.de/receive/zimport_mods_00002652.

[4] Jäger, R. (2022). Multisensornavigation, Georeferenzierung und SLAM auf Bayes'scher Grundlage – Grundlagen und Systementwicklungen. Tagungsband. 213. DVW-Seminar "MST 2022 – Multisensortechnologie: Von (A)nwendungen bis (Z)ukunftstechnologien". 26., 27. September 2022. Wittwer Verlag. Buchbeitrag. 15 Seiten. https://geodaesie.info/sr/mst-2022-multisensortechnologie-von-anwendungen-bis-zukunftstechnologien/8833/4870

[5] Jäger, R., Müller, T., Saler, H. (2023). Klassische und robuste Ausgleichungsverfahren. Ein Leitfaden für Ausbildung und Praxis von Geodäten und Geoinformatikern (In German) 2. Extended Edition. To appear 10/2023. Wichmann. ISBN 978-3-87907-615-4.

APPLICATION OF SURFACE MODELS IN CRISIS MANAGEMENT

Celms Armands[1], **Ratkevičs Aivars**[1], **Puķīte Vivita**[1], **Brinkmanis-Brimanis Miks**[1, 2]

[1] *Latvian University of Life Sciences and Tehnologies*
[2] *Geo Jūrmala Ltd*
E-mail: aivars.ratkevics@lbtu.lv

When the threat of a crisis formed, it transforms into the development of the crisis and when it moves into the phases of escalation, the spatial situation of the specific event area should be considered as an important influencing factor. The impact of the spatial situation is very individual for a specific area of crisis development, while maintaining many unifying elements of the nature of the impact also in different cases. Using the knowledges of a specific spatial situation, the crisis management staff prepares and makes decisions for predicting crises, limiting their development and escalation, as well as for the organization of coping processes.

In the last two centuries, the best-known documents of territorial knowledge were the cartographic materials of territories, which can be considered as the results of territory modeling in two-dimensional planes of the territory of the area in plans and topographic maps. However, at the same time, when it was possible, three-dimensional terrain models of the territories were also requested, created and used. Their creation was time-consuming and limited in use, but they offered well-presented and understandable territory models.

As digital technologies integrate with mapping technologies, the creation and use of three-dimensional terrain situation models began to improve and expand significantly, offering new opportunities for crisis management.

The development of modeling created opportunities for users to visually evaluate the situation of the area and its impact possibilities in a 3D view, to make accurate measurements and to use automated or semi-automated analytical functions on computers. The opportunities for crisis management to provide themselves with more complete forecasts and action justifications for decision-making increased. For monitoring the development of the situation, the use of modeling options offers a significant value of quality and timesavings.

Development of situation the use of three-dimensional terrain digital models in crisis management measures is in dynamic development. It is significantly limited by the requirements for safe and proven solutions, which today's developments, prototypes and capabilities cannot yet support with a large history of experience and safety testing.

However, when dealing with the integration of 3D models in crisis management processes, there is an intensive work of specialists in the development of specific solutions and safety tests of their use. These activities are also limited by the acute lack of availability of fully trained geoinformation specialists – a shortage.

MOMENT TENSOR SOLUTION FROM WAVEFORMS OF THE EARTHQUAKES IN CENTRAL LESSER ANTILLES

Dmytro Malytskyy[1], **Andriy Gnyp**[1], **Oleksandra Astashkina**[1], **Ruslan Pak**[1], **Sergey Kravets**[1], **Vasyl Ihnatyshyn**[2], **Nataliia Zabrodska**[1]

[1] *Carpathian Branch of Subbotin Institute of Geophysics, National Academy of Sciences of Ukraine, 3-b Naukova str., 79060 Lviv, Ukraine*

[2] *Institute of Geophysics, National Academy of Sciences of Ukraine, Ferenc Rákóczi II. Transcarpathian Hungarian Institute, Kossuth square, 6. 90202 Berehove, Ukraine*

E-mail: dmalytskyy@gmail.com

In the paper, a method is presented for moment tensor inversion of only direct waveforms registered at only limited number of seismic stations. The method is based on an inversion approach described in [3, 4] where a version of matrix method has been developed for calculation of direct waves in horizontally layered half-space from the point source represented by its moment tensor. The inversion scheme consists of two steps. First (forward modeling), propagation of seismic waves in vertically inhomogeneous media is considered and a version of matrix method for calculation of synthetic seismograms on the upper surface of the horizontally layered isotropic medium is developed. The point source is located inside a layer and is represented by seismic moment tensor. The displacements on the upper surface are presented in matrix form in frequency and wave number domain, separately for far-field and near-field [4]. Subsequently, only the far-field displacements are considered and the wavefield from only direct P- and S-waves is isolated with application of eigenvector analysis reducing the problem to system of linear equations [4]. Subsequently (inverse modeling), spectra of the moment rate tensor components are calculated using a solution of generalized inversion and transformed to time domain by applying the inverse Fourier transform. The 1D crustal model used in all the inversions of waveforms is listed in Table 1. The duration of direct waves at the stations is estimated visually from the records, and accounting for the delays of reflection-conversion phases at the station corresponding to the model (Table 1) at a respective epicentral distance and source depth. As a rule, the duration of direct P-waves approximately varies between 0.3 s and 1.2 s. The highest frequency, on the other hand, is controlled by assumption of the point source and corresponds to a wavelength larger than linear dimensions of the fault, often less than 1 km in small earthquakes.

Table 1. The 1D crustal model used in the inversion of waveforms (Gonzalez et al. 2017)

Thickness, km	Velocity V_p, km/s	Velocity V_s, km/s	ρ, kg/m^3
3	3.5	1.99	2318
12	6.0	3.41	2717
15	7.0	3.98	2968
190	8.0	4.55	3291

Using the method presented in the current paper focal mechanisms of four small earthquakes in the Central Lesser Antilles are retrieved. The mechanisms independently determined for the same earthquake from its waveforms at different single stations turned out almost identical. The mechanisms are also compared with focal mechanisms estimated by full waveform inversion [1]. A conclusion is drawn out that the method will be useful when focal mechanisms can't be obtained by other methods, the problem typical for regions with low seismicity and insufficient number of seismic stations.

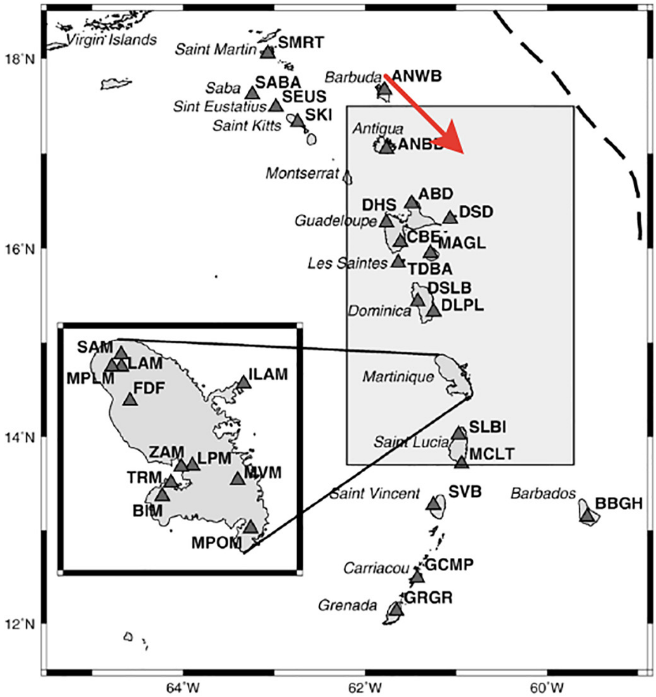

Fig. 1. Map of the stations (triangles) used for determining the moment tensor solutions

As result, we first propose to compare the mechanisms independently determined for the same earthquake from its waveforms at different single stations. For the earthquake of 2014-05-14 they turn out almost indistinguishable between the stations SAM, SLBI, ILAM and SAM, SLBI, ILAM, MPOM (Fig. 1) and only slightly differ from the mechanism estimated by full waveform inversion (event 10, [1]), the same as for the earthquake of 2013-10-24 between the station ABD and stations ABD, DHS, DSD (event 5, [1]), which at least means that despite all the uncertainties the unique solution exists and is reproducible. Finally, the focal mechanism solutions for the two earthquakes: 2014-08-09 and 2013-10-18 determined here by inversion of direct waveforms are compared to those estimated by full waveform inversion (events 21 and 3, [1]). Larger differences however are present between the nodal planes for these earthquakes. There again a number of reasons may be why the solutions turn out different, the solutions estimated for small earthquakes by full waveform inversion also prone to a set of uncertainties. The subject deserves wider and deeper discussion, beyond however the frames of the present paper.

References

[1] Gonzalez, O., Clouard, V., Zahradnik, J. (2017). Moment tensor solution along the central Lesser Antilles using regional broadband stations. *Tectonophysics, 717*, 214–225.

[2] Mai, M., Schorlemmer, D., Page, M. et al. (2016). The Earthquake-Source Inversion Validation (SIV) Project. *Seismological Research Letters*, 87(3), 690–708.

[3] Malytskyy, D. (2010). Analytic-numerical approaches to the calculation of seismic moment tensor as a function of time. *Geoinformatika, 1*, 79–85. (In Ukrainian)

[4] Malytskyy, D. (2016). Mathematical modeling in the problems of seismology. *Naukova Dumka*, p. 277. (In Ukrainian).

THE 1884 SLR STATION IN RIGA: A REVIEW OF THE CURRENT SITUATION

Kalvis Salmiņš, Jānis Kauliņš, Jorge del Pino Boytel

University of Latvia, Institute of Astronomy, Jelgavas str. 3, Riga, Latvia
E-mail: kalvis.salmins@lu.lv

The SLR station 1884 Riga started in 2021 a process of upgrading several components of the SLR system and adding new components and capabilities. The new local ties have been measured, replacing the 1996 solution. A full recalibration of the SLR system was performed using the latest local ties. The new ITRF2020 coordinate solution for the SLR 1884 Riga is significantly improved in relation to the ITRF2008 and ITRF2014 solutions. This is a consequence of the new hardware (multichannel detector unit, photometry unit and telescope driving system) introduced, the improvement of operation procedures, both software and operators training, and the full and regular system calibrations carried out since 2014. The 2023 results show that our system currently has a short range bias stability of the order of 1 cm or less, a precision of < 5 mm and the current Lageos normal point RMS is 3.1 mm. These results put our station among the well-performing systems in the ILRS global network producing high quality data. We present an overview of the latest developments in satellite photometry and event timing.

TWO-YEAR LONG DIGITAL ZENITH CAMERA VESTA DEFLECTION OF VERTICAL MEASUREMENTS AT THE TEST SITE

Inese Varna, Ansis Zarins, Augusts Rubans

University of Latvia, Institute of Geodesy and Geoinformatics, Jelgavas str. 3, Riga, Latvia
E-mail: inese.varna@lu.lv

In 2016 design of a digital zenith camera (DZC) (named VESTA – VErtical by STArs) for deflection of vertical (DoV) component measurements was completed in the Institute of Geodesy and Geoinformatics (GGI) of the University of Latvia [1]. The DoV at a point on the Earth is a measure of how much gravity normal has been inclined by local anomalies such as terrain and geological features. Several units of VESTA have been developed and assembled in GGI, series of successful observations have been performed and applied for calculation of regional quasi-geoid parameters [2]. In 2019 one unit after international tender was sold to the Louisiana State University (USA) and is successfully working there.

Differently from other known DZCs [3, 4, 5, 6], VESTA is a highly portable instrument (12 kg, mounted on a light tripod) and can be operated by a single person. It consists of a small (16 inch) vertically oriented telescope with a CCD camera and attached computer-controlled focuser, mounted on a rotating levelable platform. All involved equipment and actuators are controlled by an on-board computer; the process of measurements is almost completely automated and requires operator intervention only for setting up. A measurement session typically includes zenith star observations in 30-90 rotation positions, usually 10 short exposure frames in each position. Star field images are complemented with high sensitivity tiltmeter data, thus providing link to both star-defined orientation in inertial coordinate system and gravity field direction. A minimal measurement session takes less than an hour and offers about 0.1 arc second DoV accuracy; longer sessions give more accurate results.

Post-processing of measurements includes analysis of star field images, automated star image identification with reference catalogue data (a subset of GAIA catalogue is currently used), calculation of apparent places of stars (using NOVAS vector astrometry package), calculation of projections of ellipsoidal zenith on CCD image, corrections for instrument tilt, and, finally, calculation of DoV. The whole process is automated and requires only minimal operator intervention.

More detailed analysis of optimal measurement conditions and error sources of DZC VESTA is currently performed. This study focuses on testing various parameters of DZC VESTA measurement session: session length, image binning, exposure time; monitoring changes of DoV values over 2-year time at the same site and considering influence of external conditions: average number of observed stars, temperature, humidity, pressure, wind speed, sky, microseismic.

For measurement purpose, a test site with 4 points at a 50x50 meter distance was established and DoV measurements by DZC VESTA were started there in May 2021. Moreover, measurements were continued for two years to obtain DoV time series at all 4 points of the test site, so currently regular measurements are completed.

Acknowledgements

This research has been supported by the European Regional Development Fund activity "Post-doctoral Research Aid", project No. 1.1.1.2/VIAA/4/20/666 "Investigation on accuracy improvement of automated zenith camera's VESTA deflection of vertical measurements".

References

[1] Zariņš, A., Rubans, A., Silabriedis, G. (2016). Digital Zenith Camera of the University of Latvia. *Geod. Cartogr.*, *42*(4), 129–135. https://doi.org/10.3846/20296991.2016.1268434.

[2] Morozova, K., Jäger, R., Zarins, A., Balodis, J., Varna, I., Silabriedis, G. (2021). Evaluation of Quasi-Geoid Model Based on Astrogeodetic Measurements: Case of Latvia. *J. Appl. Geod.*, *15*(4), 319–327. https://doi.org/10.1515/jag-2021-0030.

[3] Hirt, C., Seeber, G. (2008). Accuracy Analysis of Vertical Deflection Data Observed with the Hannover Digital Zenith Camera System TZK2-D. *J. Geod.*, *82*(6), 347–356. https://doi.org/10.1007/s00190-007-0184-7.

[4] Tian, L., Guo, J., Han, Y., Lu, X., Liu, W., Wang, Z., Wang, B., Yin, Z., Wang, H. (2014). Digital Zenith Telescope Prototype of China. *Chinese Sci. Bull.*, *59* 17), 1978–1983. https://doi.org/10.1007/s11434-014-0256-z.

[5] Halicioglu, K., Deniz, R., Ozener, H. (2016). Digital Astro-Geodetic Camera System for the Measurement of the Deflections of the Vertical: Tests and Results. *Int. J. Digit. Earth*, *9*(9), 914–923. https://doi.org/10.1080/17538947.2016.1189612.

[6] Varna, I., Willi, D., Guillaume, S., Albayrak, M., Zarins, A., Ozen, M. (2023). Comparative Measurements of Astrogeodetic Deflection of the Vertical by Latvian and Swiss Digital Zenith Cameras. *Remote Sensing, 15*(8), 2166. https://doi.org/10.3390/rs15082166.

ACCURACY IMPROVEMENT OF THE ASTROGEODETIC MEASUREMENTS AND DEVELOPMENT OF THEIR DUAL APPLICATION

Ingus Mitrofanovs, Inese Vārna, Ansis Zariņš, Augusts Rubans, Irīna Baltmane

University of Latvia, Institute of Geodesy and Geoinformatics, Jelgavas str. 3, Riga, Latvia

The goal of the project is to Improve existing astrogeodetic measurement methods of the institute of geodesy and geoinformatics and adapt them for possible dual applications.

The results of the project will help understanding the effect of anomalous refraction on vertical deflection measurements performed with a digital zenith camera (DZC).

To achieve the highest possible level of accuracy of DZC measurements, efforts should be made to eliminate or minimize the effects of error-causing factors such as anomalous refraction. Studies have been conducted around the world to explain anomalous refraction, as it is a major source of error in astrometric observations. A particularly extensive study has been conducted by Taylor and presented in [1]. Possible causes of anomalous refraction include the rippling of atmosphere layers with different density, horizontal gradients of atmospheric layer density, and others, but there is no conclusive explanation for the origin of anomalous refraction. However, it is very likely that its origin could be up to a height of 60 m above the ground.

Within the framework of the project, several meteo sensors and a drone (UAV) for lifting the meteo sensor to a height of up to 100 m have been purchased. Typically, one DZC measurement session lasts 45–70 minutes (average about 50). This is the time required to "hold" the meteo sensor in the air to obtain information about the atmospheric processes taking place during the measurement session.

A space object optical tracking system for positional astrometric observations has been developed at the LU GGI. Currently, the first optical observations of satellites (geostationary and flying in high Earth orbits (above ~10,000 km)) have been made. Evaluation of the alternative system applications showed that it is possible to adapt the image processing and analysis and mechatronics control algorithms used to process images of space objects and track their trajectories. New application is possible – optical identification of low-flying objects such as drones, by searching objects in the sky background images by specific colour, contrast, configuration, and motion. The drone purchased within the framework of the proposed project will be used to develop a low-flying object identification solution.

Within the project it is planned to perform:

- Recording of meteo parameters during DZC VESTA measurements;
- Processing and interpretation of the obtained data, development of recommendations – describe conditions under which it is possible to minimize the impact of anomalous refraction;
- Development and adaptation of optical object identification software for various tasks;
- Acquisition of optical images of low-flying objects for testing identification software.

The recommendations developed during the project will be used not only by LU GGI researchers performing vertical deflection measurements with VESTA, but also by users of other zenith cameras in the world.

The achieved results will be the basis for higher technological readiness level (TRL) research for the development of solutions for the identification of moving objects. The implementation of the project will increase the competence and competitiveness of researchers at the University of Latvia at the international level, facilitating the attraction of foreign funding and involvement in international scientific cooperation projects. The equipment purchased for the implementation of the project after the project will be used to ensure and strengthen the research capacity of the LU GGI, as well as to serve for the preparation and implementation of other research and applied project applications.

The research and methodology developed during the project will be applied in future measurements of zenith cameras. International cooperation in this field will be encouraged.

Acknowledgements

Project “Accuracy improvement of the astrogeodetic measurements and development of their dual application” is carried out thanks to the donation of “MikroTik”, which is administered by the University of Latvia Foundation.

References

[1] Taylor, M. S. et al. (2013). On the source of astrometric anomalous refraction. *Astron. J.,* 145(3), 82. https://doi.org/10.1088/0004-6256/145/3/82.

ANOMALOUS REFRACTION AND ITS INFLUENCE ON DIGITAL ZENITH CAMERA MEASUREMENTS

Inese Varna, Ansis Zarins, Augusts Rubans, Ingus Mitrofanovs

University of Latvia, Institute of Geodesy and Geoinformatics, Jelgavas str. 3, Riga, Latvia
E-mail: inese.varna@lu.lv

Atmospheric refraction is a phenomenon that occurs when light travels through the Earth's atmosphere. It is causing the apparent position of objects in the sky to appear slightly different from their true position, especially when they are near the horizon. Under normal conditions, atmospheric refraction should follow the laws of geometric optics and, knowing parameters of Earth's atmosphere, could be predicted using standard atmospheric refraction models.

However, anomalous refraction can occur under certain conditions, leading to deviations from the predicted refraction. Anomalous refraction in the atmosphere is caused by variations in the temperature and pressure of the air, which can lead to changes in the refractive index of the atmosphere.

Anomalous refraction is the main limiting factor of ground-based astrometric observation's precision, causing low-frequency irregular angular displacements of observed stars.

One of such observation types where anomalous refraction interferes with observation results are deflection of vertical measurements by digital zenith cameras (DZC). Deflection of vertical (DoV) is the angle between the direction of the gravity vector (plumbline) at a point on the Earth's surface and the ellipsoid's normal through the same point. Therefore, DoVs characterise the direction of Earth's gravity field and can be used for, e.g., geoid determination. DZCs use image coordinates of observed stars at the zenith direction and star catalogue data as high accuracy reference for DoV determination.

According to standard atmospheric refraction models, there should be no refraction effect at the zenith direction. However, anomalous refraction still exists at the zenith direction and affects also observations of DZCs.

Comprehensive study of Taylor et al. [1] on anomalous refraction impact on astrometric observations has approved that it ubiquitous and it is not directly dependent on ground weather conditions (temperature, wind speed, pressure). No correlation was found between simultaneous observations with two or even three closely located telescopes in TDI mode (Time-Delay and Integrate CCD readout or drift-scan mode). Taylor et al. concludes that source of anomalous refraction is at low heights (~10–100 m) and physical scale of involved turbulence cells is small (~2 m), and proposes a hypothesis that anomalous refraction might be caused by an atmospheric disturbance created by the dome or telescope itself or it is a result of the integration of quasi-stochastic atmospheric dynamics over the entire air column, with the greatest contributions originating in the surface layer.

Anomalous refraction has also been observed as an error source in several studies employing DZCs [2, 3, 4, 5]. Hirt [2] has used observations collected in the single site for 6 nights which is the only study of anomalous refraction using DZC. This study concludes that the anomalous refraction effect at the zenith reaches from 0.05 arcseconds up to about 0.2 arcseconds.

Attempt to understand anomalous refraction by using DZC VESTA (VErtical by STArs) of University of Latvia has been done by performing DZC VESTA observations at test site with four points during two-year time. Overnight (5–10 h long) observations were done during all seasons over various weather conditions. Initially one meteo-sensor measuring temperature, atmospheric pressure and relative humidity was installed on DZC VESTA.

The amplitudes of the observed zenith coordinate fluctuations reach several arcseconds, and the amplitudes of the final DoV values are within ~0.2–0.5 arcseconds during overnight session. Warm weather front passing observation site caused high DoV amplitudes of ~0.5 arcseconds. For comparison, accuracy of DZC VESTA DoV values is 0.1 arcsecond for typical session of 45–60 minutes. DoV observations performed during warmer weather of summer months tend to have higher residuals. Apart from that, no correlation was found between result DoV residuals and atmospheric pressure.

Acknowledgements

This research has been supported by the European Regional Development Fund activity “Post-doctoral Research Aid”, project No. 1.1.1.2/VIAA/4/20/666 “Investigation on accuracy improvement of automated zenith camera’s VESTA deflection of vertical measurements”.

Project “Accuracy improvement of the astrogeodetic measurements and development of their dual application” is carried out thanks to the donation of “MikroTik”, which is administered by the University of Latvia Foundation.

References

[1] Taylor, M. S., McGraw, J. T., Zimmer, P. C., Pier, J. R. (2013). On the Source of Astrometric Anomalous Refraction. *Astron. J.*, *145*(3). https://doi.org/10.1088/0004-6256/145/3/82.

[2] Hirt, C. (2006). Monitoring and Analysis of Anomalous Refraction Using a Digital Zenith Zamera System. *Astron. Astrophys.*, *459*(1), 283–290. https://doi.org/10.1051/0004-6361:20065485.

[3] Hirt, C., Seeber, G. (2008). Accuracy Analysis of Vertical Deflection Data Observed with the Hannover Digital Zenith Camera System TZK2-D. *J. Geod.*, *82*(6), 347–356. https://doi.org/10.1007/s00190-007-0184-7.

[4] Hirt, C., Bürki, B., Somieski, A., Seeber, G. (2010). Modern Determination of Vertical Deflections Using Digital Zenith Cameras. *J. Surv. Eng.*, *136*(1), 1–12. https://doi.org/10.1061/(ASCE)SU.1943-5428.0000009.

[5] Guillaume, S. (2015). Determination of a Precise Gravity Field for the CLIC Feasibility Studies, PhD Thesis. Eidgenössische Technische Hochschule ETH Zürich. https://doi.org/https://doi.org/10.3929/ethz-a-010549038.

TOWARDS WELL-BEING CONCEPT BASED ON ENVIRONMENTAL DATA, GEOSPATIAL DATA AND DYNAMIC MODELLING

Ieva Vitolina[1], **Una Krutova**[2], **Janis Kapenieks Sen.**, **Alesandrs Gorbunovs**, **Janis Kapenieks Jun.**, **Atis Kapenieks**, **Jean-Denis Mathias**[3]

[1]*Riga Technical University, Distance Education Study Centre, Kronvalda boulv. 1, Riga, Latvia*
[2]*Riga Technical University, Faculty of Civil Engineering, Institute of Transport Engineering, Department of Geomatics, Kipsalas Street 6A, Riga, Latvia*
[3]*National Research Institute for Agriculture, Food and Environment, 9 Av. Blaise Pascal, 63170 Aubière, Clermont-Ferrand, France*
E-mail: ieva.vitolina@rtu.lv

Riga Technical University coordinates the Horizon Europe project "Twinning in Environmental Data and Dynamical Systems Modelling for Latvia (TED4LAT)", which started in October 2022 and will last 36 months. TED4LAT is a Coordination and Support Action project targeting the overarching objective: Twinning to reach high international standards in research and innovation in Latvia. TED4LAT will be implemented by twinning two prominent research institutions in France, National Research Institute for Agriculture, Food and Environment (INRAE), and in Italy, the Polytechnic University of Turin (POLITO), with three widening Latvian Universities (Liepaja University, Vidzeme University of Applied Sciences, and Riga Technical University). The Baltic Open Solutions Center, a Latvian SME, joins the endeavour as a living-lab application partner. TED4LAT envisages implementing a joint multidisciplinary research agenda in the area of Data Science and Dynamic System modelling.

A common TED4LAT research agenda will address scientific challenges related to the use of satellite data for environmental applications, as accompanying measures, computational infrastructure upgrades, doctoral schools, workshops, exchange visits and seminars will be implemented. The TED4LAT research agenda, which is currently under development, includes several directions of research related to environmental data. Riga Technical University will study well-being of small towns and rural areas in Latvia. Liepaja University will focus on educational research, which includes development of artificial intelligence-enhanced competence framework on digital skills, as well as environmental sustainability big data in digital learning platforms. Vidzeme University of Applied Sciences' research will be related to integrated processing technology of multispectral images, sensors and geospatial data for precision agriculture. The TED4LAT outcomes will be important to increase the ability and capacity of Latvian universities to carry out large-scale and high-quality research in the aforementioned domains. Capacity building will result in the emergence of Latvian universities' excellence for proactively cooperating in EU research programmes over the coming decade.

Riga Technical University has started with a systematic review on well-being concept based on environmental data, geospatial data and dynamic modelling. The aim of the study is to conduct a literature review on the concept of well-being monitoring and to highlight criteria impacting well-being, the data sources and models used for characterising well-being processes. The focus of the well-being research is from the aspect of interaction between people and the environment.

According to previously defined keywords, documents from the following databases were selected for the study: Scopus (78 results), Web of Science (147 results). 87 articles were determined to be relevant for the performing of a systematic review report.

Although the systematic review is still in process, for the moment it is possible to draw some conclusions: (1) The dominant approach is anthropocentric approach (ecosystem, nature is a tool or service for human well-being). A holistic approach (human as ecosystem part) or an ecocentric approach does not dominate as a research goal in the documents. (2) Well-being is mainly determined at the national or regional level, not measured for small territories (local scale). (3) The concept of well-being is interpreted through a combination of different criteria and indicators depending on the context and the goals of the research authors. Mainly criteria and indicators are grouped to characterise: economic, social, human and environmental aspects.

The planned further works are as follows: (1) To continue to perform systematic review related to well-being concept, to synthesise the results. (2) To focus on local scale research used geolocalized well-being factors. (3) To draw conclusions about approaches and dynamic data modelling useful for Latvia. (4) Identify new approaches based on technologies for well-being data collection and analysis such as satellite imaging analysis.

Acknowledgements

This research has been funded by the European Union. Project "Twinning in Environmental Data and Dynamical Systems Modelling for Latvia". TED4LAT, No. 101079206. Views and opinions expressed are however those of the author(s) only and do not necessarily reflect those of the European Union or European Research Executive Agency. Neither the European Union nor European Research Executive Agency can be held responsible for them.